Crater function approach to ion-induced nanoscale pattern formation: Craters for flat surfaces are insufficient

Matt P. Harrison and R. Mark Bradley
Department of Physics, Colorado State University, Fort Collins, Colorado 80523, USA
(Received 7 February 2014; revised manuscript received 3 April 2014; published 2 June 2014)

In the crater function approach to the erosion of a solid surface by a broad ion beam, the average crater produced by the impact of an ion is used to compute the constant coefficients in the continuum equation of motion for the surface. We extend the crater function formalism so that it includes the dependence of the crater on the curvature of the surface at the point of impact. We then demonstrate that our formalism yields the correct coefficients for the Sigmund model of ion sputtering if terms up to second order in the spatial derivatives are retained. In contrast, if the curvature dependence of the crater is neglected, the coefficients can deviate substantially from their exact values. Our results show that accurately estimating the coefficients using craters obtained from molecular dynamics simulations will require significantly more computational power than was previously thought.

DOI: 10.1103/PhysRevB.89.245401 PACS number(s): 81.16.Rf, 79.20.Rf, 68.35.Ct

I. INTRODUCTION

Bombarding a solid surface with a broad ion beam can lead to the spontaneous formation of nanoscale patterns on the surface [1]. These patterns include periodic height modulations or "ripples" as well as nanodots arranged in hexagonal arrays of surprising regularity [2–7]. This has spurred widespread interest in the development of ion sputtering as a means of nanofabrication. Since broad beam ion bombardment is relatively easy to implement, the potential for cost-effective mass production of nanostructures is quite high.

Much of the theoretical work performed in analyzing these patterns has been based on the continuum Bradley-Harper (BH) theory [8], which is itself based on the Sigmund model of ion sputtering [9]. BH showed that for the Sigmund model the sputter yield at a point on the surface does not just depend on the local angle of incidence—it depends on the surface curvature as well. Because high points on the surface are eroded more slowly than the low points, the curvature dependence of the sputter yield leads to an instability of the solid surface. The BH theory has been extended to include nonlinear effects [10–13], and so it applies to binary materials [14].

Since the work of Carter and Vishnyakov (CV) in 1996 [15], it has become increasingly clear that ion-induced mass redistribution can play an important role in the pattern formation [16–29]. In this process, momentum is transferred from the incident ions to atoms near the surface of the solid. These atoms are not ejected from the solid surface as they would be in sputtering. Instead, they are displaced within the solid.

The theories of BH and of CV are based on simple models of sputtering and mass redistribution. It has been unclear just how good these models are and in what circumstances they can be reasonably applied. Moreover, the predictions of the BH and CV theories depend on a number of phenomenological parameters but give no means of computing their values.

Recently, there has been considerable interest in incorporating the results of molecular dynamics (MD) simulations into a continuum theory of ion-induced surface dynamics. The so-called crater function formalism (CFF) utilizes the average result of many ion impacts at a single point to generate a Green's function, which is then used to determine the response of a surface to bombardment with a broad ion beam [21,30,31]. This approach has the advantage that it takes into account both sputtering and ion-induced mass redistribution and does not rely on simple models of these phenomena. The formalism yields estimates of the constant coefficients that appear in the continuum equation of motion based on input from MD simulations. In the first application of this method to a specific physical problem, Norris *et al.* carried out MD simulations of the bombardment of a silicon surface with 100 and 250 eV Ar^+ ions and then used their CFF to obtain estimates of some of the coefficients in the equation of motion [21].

The Green's function, which is usually referred to as the crater function, depends on the complete shape of the surface surrounding the impact point [30]. However, because it is not possible to find the crater function for an arbitrarily shaped surface using MD, the shape dependence of the crater was simply neglected in the study of Norris *et al.* that concerns the erosion of Si with an Ar^+ beam [21]. In particular, the crater function for a *flat* surface was used to estimate the coefficients in the equation of motion (EOM), even though the accuracy of such a procedure is questionable. The dependence of the crater on the shape of the surface has also been neglected in more recent applications of the CFF [32,33].

In this paper, we extend the CFF so that it includes the dependence of the crater function on the curvature of the surface at the point of impact. We give explicit expressions for the coefficients in the equation of motion which reduce to the expressions given by Norris *et al.* [21] only if the curvature dependence of the crater function is neglected. We then demonstrate that our extended CFF yields the exact BH coefficients for the Sigmund model. In contrast, the BH coefficients are not recovered if the curvature dependence of the crater function is neglected. This uncontrolled approximation instead results in coefficients that are off by a factor of 2 for normal-incidence bombardment. Our results therefore strongly suggest that if reliable estimates of the coefficient values are to be obtained using the CFF, the curvature dependence of the crater function must be taken into account.

This paper is organized as follows. We introduce the crater function and its arguments in Sec. II. In Sec. III, we use the

crater function to determine the coefficients in the EOM for the special case in which the surface height does not vary in the direction transverse to the plane of the beam. In Sec. IV, we develop the geometric preliminaries required to extend our theory to fully three-dimensional (3D) surfaces. Section V generalizes the results of Sec. III to the case in which the surface height varies in both the transverse and the longitudinal directions. Section VI contains an explicit demonstration that our extended CFF is in accord with the BH theory in the case of the Sigmund crater. In Sec. VII, we compare our theory to the CFF of Norris *et al.* [21] and demonstrate that for the Sigmund crater the latter produces coefficients that can differ significantly from their exact values. Additionally, we discuss the implications of our work and place its results in context. Our findings are summarized in Sec. VIII.

II. THE CRATER FUNCTION

Consider the bombardment of a solid elemental material with a broad ion beam. We will assume that the material is amorphous or, if it is crystalline, that a layer at the surface of the solid is rendered amorphous by the ion bombardment. The sample surface will be taken to be nominally flat before the irradiation begins.

We define the $\hat{\boldsymbol{z}}$ direction to be the global vertical, normal to the macroscopic surface. $\hat{\boldsymbol{x}}$ is taken to be the direction of the projection of the incident ion beam onto the macroscopic surface, and $\hat{\boldsymbol{y}}$ is taken to be normal to the x-z plane. The incident ion flux is $\boldsymbol{J} = J(\hat{\boldsymbol{x}} \sin\theta - \hat{\boldsymbol{z}} \cos\theta)$, where the angle of incidence θ is the angle between the global vertical and the incident beam, as shown in Fig. 1. An arbitrary point on the surface **P** is given by $\boldsymbol{r} = x\hat{\boldsymbol{x}} + y\hat{\boldsymbol{y}} + h(x,y)\hat{\boldsymbol{z}}$, where $h(x,y)$ is the height of the point above the x-y plane. (For convenience, we will suppress the time dependence of h unless it is necessary to explicitly display it.)

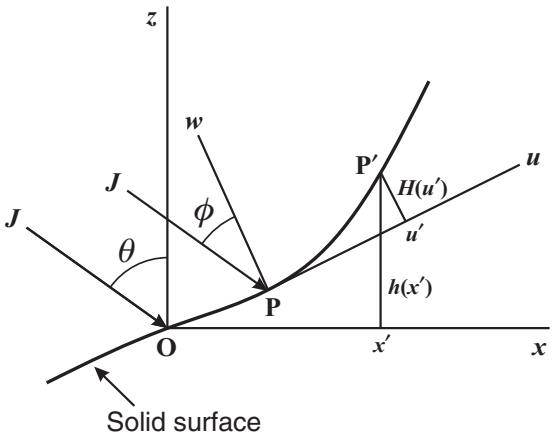

FIG. 1. The solid surface at time t. Points **O**, **P**, and **P**′ lie on the surface. The global frame of reference has its origin at **O** and has axes x, y and z, whereas the local frame of reference has its origin at **P** and has axes u, v, and w. $\boldsymbol{J}$ is the incident ion flux. θ and ϕ are the global and local angles of incidence, respectively. The height of point **P**′ is $h(x')$ in the global frame but is $H(u')$ in the local frame. For simplicity, the figure has been drawn for the special case in which $h(x,y)$ is independent of y.

Our goal is to evaluate $\partial h/\partial t$ at an arbitrary point **O** on the solid surface at an arbitrary time $t > 0$. To that end, we will place the global origin at the position of **O** at time t, as shown in Fig. 1. The global origin will be taken to be stationary, and it so will remain fixed as the surface point **O** moves either up or down.

The collision cascade that an impinging ion produces in the solid has a characteristic lateral length scale that we will denote by l. We will assume that a smoothing mechanism ensures that the surface height varies only a little over this length scale; in practice, the smoothing mechanism could be thermally activated surface diffusion (as in the BH theory) or ion-induced viscous flow within a thin surface layer [34]. It is important to note that the equation of motion we will derive will *not* include the effects of the smoothing mechanism since we will include only terms up to second order in the wave number k and the smoothing mechanism produces terms of order k^4.

Our first step in finding the surface velocity at **O** will be to determine the contribution to it coming from ions striking the surface an arbitrary surface point **P**. In fact, we may restrict our attention to points **P** that have a distance to **O** that is on the order of a few times l or less because ions arriving at more remote points make a negligible contribution to the value of $\partial h/\partial t$ for $x = y = 0$. The height h is small for these points **P**. We will accordingly work to first order in h and its spatial derivatives throughout the remainder of the paper.

In addition to the global coordinates x, y and z, it is convenient to introduce a set of local coordinates whose origin is point **P**. Following Norris, Brenner, and Aziz [30] we define the vector $\hat{\boldsymbol{n}}$ to be the local surface normal at **P** and $\hat{\boldsymbol{t}}_u$ to be the local downbeam direction projected onto the surface. Explicitly,

$$\hat{\boldsymbol{n}} = \frac{\hat{\boldsymbol{z}} - \boldsymbol{\nabla} h}{\sqrt{1 + (\boldsymbol{\nabla} h)^2}}, \tag{1}$$

and

$$\hat{\boldsymbol{t}}_u = \frac{-\boldsymbol{J} + (\boldsymbol{J}\cdot\hat{\boldsymbol{n}})\hat{\boldsymbol{n}}}{|-\boldsymbol{J} + (\boldsymbol{J}\cdot\hat{\boldsymbol{n}})\hat{\boldsymbol{n}}|}. \tag{2}$$

$\hat{\boldsymbol{t}}_v$ is defined to be the cross product of $\hat{\boldsymbol{n}}$ and $\hat{\boldsymbol{t}}_u$. The unit vectors $\hat{\boldsymbol{n}}$, $\hat{\boldsymbol{t}}_u$, and $\hat{\boldsymbol{t}}_v$ form an orthonormal basis, and $\hat{\boldsymbol{t}}_u$ and $\hat{\boldsymbol{t}}_v$ are tangent to the surface at **P**. The local angle of ion incidence, which will be denoted by ϕ, is given by $J\cos\phi = -\boldsymbol{J}\cdot\hat{\boldsymbol{n}}$. To first order in the spatial derivatives of the surface height,

$$\phi(x,y) = \theta - h_x(x,y), \tag{3}$$

where the subscript denotes a partial derivative with respect to x. Finally, we define u, v, and w to be the coordinates along directions $\hat{\boldsymbol{t}}_u$, $\hat{\boldsymbol{t}}_v$, and $\hat{\boldsymbol{n}}$, respectively.

For surface points that have a distance to **O** that is on the order of l, we may approximate h by discarding terms of third order and higher from its Taylor series: We set $x_1 = x$, $x_2 = y$, and

$$h(x,y) = S_1 x + S_2 y + \tfrac{1}{2}K_{11}x^2 + K_{12}xy + \tfrac{1}{2}K_{22}y^2, \tag{4}$$

where

$$S_i \equiv \frac{\partial h}{\partial x_i}(0,0), \tag{5}$$

and

$$K_{ij} \equiv \frac{\partial^2 h}{\partial x_i \partial x_j}(0,0) \tag{6}$$

for $i,j = 1,2$. Although an arbitrary number of terms in the expansion (4) could in principle be retained, we will only keep terms up to quadratic order in x and y because the length scale of the height variation is assumed to be much larger than l. Note that the quantities S_i and K_{ij} are both of first order in h. This will be exploited later in our analysis.

We may also parametrize the surface in terms of the local coordinates u, v, and w. Close to **P**, the height of the solid surface above the u-v plane is given by

$$H(u,v) = \tfrac{1}{2}E_{11}u^2 + E_{12}uv + \tfrac{1}{2}E_{22}v^2, \tag{7}$$

to second order in u and v. Here

$$E_{ij} \equiv \frac{\partial^2 H}{\partial u_i \partial u_j}(0,0), \tag{8}$$

where $u_1 \equiv u$, $u_2 \equiv v$, and $i,j = 1,2$. Terms that are linear in u and v do not appear on the right-hand side of Eq. (8) because the u and v axes are tangent to the solid surface at point **P**. The expansion (7) gives a good approximation to the value of H for **O** because the distance between **O** and **P** is of order l.

We now introduce the crater function

$$F = F(u,v,\phi,E_{11},E_{12},E_{22}), \tag{9}$$

which is defined to be minus the average change in the local surface height H above the point (u,v) in the u-v plane as a result of a single ion impact at $u = v = 0$, i.e., point **P**. Although two impacts may produce very different craters, by taking the statistical average of a great number of craters, we develop an expected response. The information required to construct F is assumed to be known *a priori* from another theory or from MD simulations.

The crater function $F(u,v,\phi,E_{11},E_{12},E_{22})$ is defined in the local coordinate system of the point of impact **P**. Its first two arguments are the lateral coordinates u and v in that coordinate system. The third argument of F is the local angle of incidence ϕ. Finally, we have included the dependence of the crater on the local curvatures E_{11}, E_{12}, and E_{22}. This dependence was neglected by Norris *et al.* [21], but, as we will discuss in Sec. VII, evidence from experiments [35] and MD simulations [36] suggests that it can have a significant effect.

Note that although the E_{ij}'s refer to second derivatives of H with respect to the local coordinates u and v at point **P**, it is shown in Sec. IV that to first order they are equal to the corresponding second derivatives of h with respect to the global coordinates x and y at point **O**, i.e.,

$$E_{ij} = K_{ij} \tag{10}$$

for $i,j = 1,2$. We may therefore rewrite Eq. (9) as

$$F = F(u,v,\phi,K_{11},K_{12},K_{22}). \tag{11}$$

III. THE EXTENDED CRATER FUNCTION FORMALISM IN TWO DIMENSIONS

The goal of our analysis is to derive an EOM of the form

$$\frac{1}{J}\frac{\partial h}{\partial t} = C_0(\theta) + C_1(\theta)h_x + C_2(\theta)h_y + C_{11}(\theta)h_{xx} + C_{12}(\theta)h_{xy} + C_{22}(\theta)h_{yy}, \tag{12}$$

and to write the coefficients $C_0, C_1, \ldots, C_{22}$ in terms of the crater function F. The first step in our analysis will be to determine the contribution to the normal velocity of the surface at **O** due to impacts at point **P**. Having found this, we will perform a flux weighted integral over all possible impact points **P** to determine the overall response.

To make the analysis as transparent as possible, we will begin by considering the special case in which the surface height h has no dependence on y. In this case, Eq. (12) reduces to

$$\frac{h_t}{J} = C_0(\theta) + C_1(\theta)h_x + C_{11}(\theta)h_{xx}, \tag{13}$$

where $h_t \equiv \partial h/\partial t$. This problem is equivalent to a two-dimensional (2D) problem in which h depends only on x and t and ions are incident in the x-z plane with an angle of incidence θ. The effective crater function for this 2D problem is

$$g(u,\phi,E_{11}) \equiv \int_{-\infty}^{\infty} F(u,v,\phi,E_{11},0,0)dy. \tag{14}$$

We will study the equivalent 2D problem for the remainder of this section.

Consider an impact at point **P** whose position in the global coordinate system is $\boldsymbol{r} = x\hat{\boldsymbol{x}} + h(x)\hat{\boldsymbol{z}}$. The lateral position of the global origin **O** in the local reference frame of the impact point is to first order

$$u = \hat{\boldsymbol{t}}_u(x)\cdot(\boldsymbol{0}-\boldsymbol{r}) = [\hat{\boldsymbol{x}} + h_x(x)\hat{\boldsymbol{z}}]\cdot[-x\hat{\boldsymbol{x}} - h(x)\hat{\boldsymbol{z}}] = -x. \tag{15}$$

Thus, to first order, we may replace the first argument of the crater function $g(u,\phi,E_{11})$ by $-x$. Similarly, the height of origin **O** relative to the local frame of the impact point **P** is to first order

$$H(u) \equiv \hat{\boldsymbol{n}}(x)\cdot(\boldsymbol{0}-\boldsymbol{r}) = [-h_x(x)\hat{\boldsymbol{x}} + \hat{\boldsymbol{z}}]\cdot[-x\hat{\boldsymbol{x}} - h(x)\hat{\boldsymbol{z}}] = xh_x(x) - h(x). \tag{16}$$

Recall that the crater function gives the change in surface height in the direction of the local normal $\hat{\boldsymbol{n}}$, and so we must project the local normal velocity along the global vertical direction in order to find the velocity of the surface point **O** along the global vertical direction. However, because

$$\hat{\boldsymbol{n}}(x)\cdot\hat{\boldsymbol{z}} = 1 \tag{17}$$

to first order, this projection has no effect on the linearized EOM we will obtain.

This analysis permits us to write the time derivative of the surface height at **O** in terms of the crater function g and the ion flux J:

$$h_t(0,t) = -J\int g(-x,\phi,E_{11})\cos\phi\, dx, \tag{18}$$

where the factor of $\cos\phi$ comes from projecting the ion flux onto the local normal at point **P**. Finally, because only points **P** within a distance on the order of l from the origin give a significant contribution to the integral on the right-hand side of Eq. (18), we may replace E_{11} by $K \equiv K_{11}$ in the integral.

We are now in a position to begin analyzing the integrand in Eq. (18). To do so, we will linearize in the quantities $S \equiv S_1$ and K, which, as we noted earlier, are first order in h. This will yield expressions for the coefficients in the EOM (13). Making use of $\phi = \theta - h_x = \theta - S - Kx$, we see that

$$\begin{aligned} -J^{-1}h_t(0,t) &= \int g(-x,\theta,0)\cos\theta\, dx \\ &\quad + S\left[\frac{d}{dS}\int g(-x,\theta - S,0)\cos(\theta - S)dx\right]\Big|_{S=0} \\ &\quad + K\left[\frac{d}{dK}\int g(-x,\theta - Kx,K)\cos(\theta - Kx)dx\right]\Big|_{K=0}. \end{aligned} \tag{19}$$

The first term on the right-hand side of Eq. (19) is particularly simple and gives the steady-state erosion velocity. Notice that we may perform a change of variable $x \to -x$ without changing the overall sign of this term, i.e.,

$$\int g(-x,\theta,0)\cos\theta\, dx = \int g(x,\theta,0)\cos\theta\, dx. \tag{20}$$

Therefore, the steady-state erosion velocity for the undisturbed flat surface is

$$V_0(\theta) = J\,\cos\theta\int g(x,\theta,0)dx. \tag{21}$$

The second term on the right-hand side of Eq. (19) is somewhat more involved. Noticing that the only dependence of g upon S comes from the the local angle of incidence ϕ, it is clear that we may write the second term on the right-hand side of Eq. (19) as

$$\begin{aligned} &S\left[\frac{d}{dS}\int g(-x,\theta - S,0)\cos(\theta - S)dx\right]\Big|_{S=0} \\ &\quad = -S\frac{\partial}{\partial\theta}\int g(x,\theta,0)\cos\theta\, dx \\ &\quad = -\frac{S}{J}\frac{\partial}{\partial\theta}V_0(\theta). \end{aligned} \tag{22}$$

Finally, we turn to the dependence of h_t on K. The last term on the right-hand side of Eq. (19) becomes

$$\begin{aligned} &K\left[\frac{d}{dK}\int g(-x,\theta - Kx,K)\cos(\theta - Kx)dx\right]\Big|_{K=0} \\ &\quad = K\int dx\left[-x\,\sin\theta g(x,\theta,0) + x\,\cos\theta\frac{\partial g}{\partial\theta}(x,\theta,0)\right. \\ &\qquad \left. + \cos\theta\frac{\partial g}{\partial K}(x,\theta,K)\Big|_{K=0}\right], \end{aligned} \tag{23}$$

where we have once again used the change of variable $x \to -x$.

Inserting Eqs. (21)–(23) into Eq. (19), we arrive at an EOM of the form (13). Defining

$$M_K(\theta) = \int g(x,\theta,K)dx, \tag{24}$$

and

$$M_x^{(n)}(\theta) = \int g(x,\theta,0)x^n dx, \tag{25}$$

we obtain

$$\begin{aligned} h_t(0,t) = &-JM_x^{(0)}\cos\theta + J\frac{\partial}{\partial\theta}\left(M_x^{(0)}\cos\theta\right)h_x(0,t) \\ &- J\left[\frac{\partial}{\partial\theta}\left(M_x^{(1)}\cos\theta\right) + \cos\theta\frac{\partial}{\partial K}M_K\Big|_{K=0}\right]h_{xx}(0,t). \end{aligned} \tag{26}$$

Comparing this to Eq. (13), we see that

$$C_0(\theta) = -M_x^{(0)}\cos\theta, \tag{27}$$

$$\begin{aligned} C_1(\theta) &= \frac{\partial}{\partial\theta}\left(M_x^{(0)}\cos\theta\right) \\ &= -\frac{\partial}{\partial\theta}C_0(\theta), \end{aligned} \tag{28}$$

and

$$C_{11}(\theta) = -\frac{\partial}{\partial\theta}\left(M_x^{(1)}\cos\theta\right) - \cos\theta\frac{\partial}{\partial K_{11}}M_{K_{11}}\Big|_{K_{11}=0}. \tag{29}$$

The first term on the right-hand side of Eq. (29) stems from the fact that a nonzero surface curvature gives rise to a local angle of ion incidence that depends on the point of impact. The second is a direct result of the curvature dependence of the crater function itself.

IV. GEOMETRIC PRELIMINARIES IN THREE DIMENSIONS

The extension of the analysis of the previous section to 3D is subtle and requires care. In this section, we delve into the relationship between the local and the global coordinate systems before turning to the CFF in 3D. As discussed in Sec. II, the local coordinate system is defined using the local surface normal and the projection of the ion beam onto the local tangent plane.

To first order in h, the local unit vectors may be expressed in terms of their global counterparts as follows:

$$\hat{\boldsymbol{t}}_u = \hat{\boldsymbol{x}} - (h_y\cot\theta)\hat{\boldsymbol{y}} + h_x\hat{\boldsymbol{z}}, \tag{30}$$

$$\hat{\boldsymbol{t}}_v = (h_y\cot\theta)\hat{\boldsymbol{x}} + \hat{\boldsymbol{y}} + h_y\hat{\boldsymbol{z}}, \tag{31}$$

and

$$\hat{\boldsymbol{n}} = -h_x\hat{\boldsymbol{x}} - h_y\hat{\boldsymbol{y}} + \hat{\boldsymbol{z}}. \tag{32}$$

The partial derivatives of h are to be evaluated at the point (x,y) in the x-y plane in these expressions. The coordinates of point **O** in the local coordinate system (u, v, and w) can now be found using Eqs. (30)–(32). The vector leading from **P** to

O is $-\boldsymbol{r}$. Recalling that $\boldsymbol{r} = x\hat{\boldsymbol{x}} + y\hat{\boldsymbol{y}} + h(x,y)\hat{\boldsymbol{z}}$, we obtain

$$u = -\boldsymbol{r}\cdot\hat{\boldsymbol{t}}_u = -x + yh_y\cot\theta, \tag{33}$$

$$v = -\boldsymbol{r}\cdot\hat{\boldsymbol{t}}_v = -y - xh_y\cot\theta, \tag{34}$$

and

$$w = -\boldsymbol{r}\cdot\hat{\boldsymbol{n}} = xh_x + yh_y - h \tag{35}$$

to first order. We may use Eq. (4) to eliminate h from Eqs. (33)–(35) because the surface height varies slowly between **O** and **P**. In particular, Eq. (35) yields

$$w = \tfrac{1}{2}K_{11}x^2 + K_{12}xy + \tfrac{1}{2}K_{22}y^2. \tag{36}$$

We are now prepared to demonstrate that Eq. (10) is valid. Inversion of Eqs. (33) and (34) gives

$$x = -u - vh_y\cot\theta, \tag{37}$$

and

$$y = -v + uh_y\cot\theta. \tag{38}$$

Since $H = w$ and the K_{ij}'s are first order in h, Eq. (36) may now be written

$$\begin{aligned} H(u,v) &= \tfrac{1}{2}K_{11}(u + vh_y\cot\theta)^2 + K_{12}(u + vh_y\cot\theta) \\ &\quad\times(v - uh_y\cot\theta) + \tfrac{1}{2}K_{22}(v - uh_y\cot\theta)^2 \\ &= \tfrac{1}{2}K_{11}u^2 + K_{12}uv + \tfrac{1}{2}K_{22}v^2. \end{aligned} \tag{39}$$

Taking the partial derivatives of H with respect to u_i and u_j, we arrive at the desired result, Eq. (10).

V. THE EXTENDED CRATER FUNCTION FORMALISM IN THREE DIMENSIONS

We will now utilize the results of Sec. IV to obtain the coefficients of the EOM in three dimensions. To extend the formalism to the general case in which the surface height depends on y as well as x, we return to the crater function $F(u,v,\phi,E_{11},E_{12},E_{22})$, the generalization of $g(u,\phi,E_{11})$ to three dimensions. The EOM is

$$h_t = -J\int dx\int dy\,\cos\phi F(u,v,\phi,E_{11},E_{12},E_{22}). \tag{40}$$

Using Eqs. (3), (10), (33), and (34), we see that this may be written

$$\begin{aligned} h_t = -J\int dx\int dy\,&\cos(\theta - h_x)F(-x + yh_y\cot\theta, \\ &-y - xh_y\cot\theta,\theta - h_x,K_{11},K_{12},K_{22}). \end{aligned} \tag{41}$$

We now expand this to linear order in h and its derivatives and let F_i denote the partial derivative of F with respect to its ith argument. This gives

$$\begin{aligned} -\frac{h_t}{J\cos\theta} = \int dx\int dy\{&F(-x,-y,\theta,0,0,0) \\ &+ F_1(-x,-y,\theta,0,0,0)(yh_y\cot\theta) \\ &+ F_2(-x,-y,\theta,0,0,0)(-xh_y\cot\theta) \\ &- \sec\theta\frac{\partial}{\partial\theta}[\cos\theta F(-x,-y,\theta,0,0,0)h_x] \\ &+ K_{11}F_4(-x,-y,\theta,0,0,0) \\ &+ K_{12}F_5(-x,-y,\theta,0,0,0) \\ &+ K_{22}F_6(-x,-y,\theta,0,0,0)\}. \end{aligned} \tag{42}$$

To simplify this expression, we will examine it term by term and will employ Eq. (4). The second term on the right-hand side of Eq. (42) is

$$\begin{aligned} I_2 \equiv \int dx\int dy\,&F_1(-x,-y,\theta,0,0,0) \\ &\times y\,\cot\theta(S_2 + K_{12}x + K_{22}y). \end{aligned} \tag{43}$$

I_2 is in fact zero. To see this, recall that we have assumed that the solid surface is amorphous. Independent of the details of the crater function $F(u,v,\phi,K_{11},K_{12},K_{22})$, therefore, symmetry demands that it be an even function of v if $K_{12} = 0$. Thus, the terms which are proportional to odd powers of y in the integrand of Eq. (43) integrate to zero. The remaining term in the integrand vanishes upon integration over x since

$$\int dx\,F_1(-x,-y,\theta,0,0,0) = F(-x,-y,\theta,0,0,0)\big|_{x=-\infty}^{x=\infty} = 0. \tag{44}$$

The third term on the right-hand side of Eq. (42) may be written

$$\begin{aligned} I_3 \equiv -\int dx\int dy\,&F_2(-x,-y,\theta,0,0,0) \\ &\times x\,\cot\theta(S_2 + K_{12}x + K_{22}y). \end{aligned} \tag{45}$$

Again using the symmetry of F, we see that $F_2(-x,-y,\theta,0,0,0)$ is an odd function of y, and thus the terms in the integrand that are proportional to even powers of y will integrate to zero. This leaves

$$\begin{aligned} I_3 &= -\cot\theta K_{22}\int dx\int dy\,F_2(-x,-y,\theta,0,0,0)xy \\ &= \cot\theta K_{22}\int dx\int dy\,F(x,y,\theta,0,0,0)x \\ &= \cot\theta K_{22}M_x^{(1)}, \end{aligned} \tag{46}$$

where we have integrated by parts and have changed the dummy variables of integration from x to $-x$ and from y to $-y$.

The fourth term on the right-hand side of Eq. (42) is identical to the analogous term in the 2D case, except that h_x now contains the additional term $K_{12}y$. However, since $F(-x,-y,\theta,0,0,0)$ is an even function of y, this term makes no contribution.

Without additional assumptions or specific information about the crater function, the fifth and seventh terms on the right-hand side of Eq. (42) cannot be simplified further. However, we may eliminate the dependence of h_t on K_{12} using a symmetry argument. Notice that a surface described by $h(x,y) = K_{12}xy$ is invariant under the transformation $y \to -y$, $K_{12} \to -K_{12}$. We may thus write

$$F(x,y,\theta,0,K_{12},0) = F(x,-y,\theta,0,-K_{12},0). \tag{47}$$

It follows that I_6, the sixth term on the right-hand side of Eq. (42), is given by

$$\frac{I_6}{K_{12}} = \left[\frac{\partial}{\partial K_{12}}\int_{-\infty}^{\infty}dx\int_{-\infty}^{\infty}dy\,F(-x,-y,\theta,0,K_{12},0)\right]\Big|_{K_{12}=0}$$
$$= \left\{\frac{\partial}{\partial K_{12}}\left[\int_{-\infty}^{\infty}dx\int_{0}^{\infty}dy\,F(-x,-y,\theta,0,K_{12},0)\right.\right.$$
$$\left.\left.+\int_{-\infty}^{\infty}dx\int_{0}^{\infty}dy\,F(-x,-y,\theta,0,-K_{12},0)\right]\right\}\Big|_{K_{12}=0}. \quad (48)$$

The quantity in the square brackets in the later expression is an even function of K_{12}. As a consequence, I_6 vanishes, and $C_{12}=0$. We could have reached this conclusion *a priori* from Eq. (12): Since the system is invariant under a reflection about the x-z plane, h_t must also remain invariant under this transformation, which implies that $C_{12}=0$.

We define

$$M_{K_{11}} = \iint F(x,y,\theta,K_{11},0,0)dx\,dy, \quad (49)$$

$$M_{K_{22}} = \iint F(x,y,\theta,0,0,K_{22})dx\,dy, \quad (50)$$

and

$$M_x^{(n)} = \iint F(x,y,\theta,0,0,0)x^n dx\,dy. \quad (51)$$

Collecting terms, we arrive at a simpler form of Eq. (42),

$$-\frac{h_t(0,0,t)}{J\,\cos\theta}$$
$$= M_x^{(0)} - S_1\sec\theta\frac{\partial}{\partial\theta}\left(\cos\theta M_x^{(0)}\right)$$
$$+K_{11}\left[\sec\theta\frac{\partial}{\partial\theta}\left(\cos\theta M_x^{(1)}\right)+\frac{\partial}{\partial K_{11}}M_{K_{11}}\Big|_{K_{11}=0}\right]$$
$$+K_{22}\left[\cot\theta M_x^{(1)}+\frac{\partial}{\partial K_{22}}M_{K_{22}}\Big|_{K_{22}=0}\right]. \quad (52)$$

Comparing this with Eq. (12), we conclude that Eqs. (27)–(29) remain valid, but the moments $M_{K_{11}}$ and $M_x^{(n)}$ are now given by Eqs. (49) and (51). We also have found that $C_2=C_{12}=0$ and that

$$C_{22}(\theta) = -\cos\theta\,\cot\theta M_x^{(1)} - \cos\theta\frac{\partial}{\partial K_{22}}M_{K_{22}}\Big|_{K_{22}=0}. \quad (53)$$

The first term on the right-hand side of Eq. (53) is present because if h_y is nonzero at the point of impact **P**, the local normal $\hat{\boldsymbol{n}}$ and the local downbeam direction $\hat{\boldsymbol{t}}_u$ have nonzero components along the y direction. The second term results from the explicit dependence of the crater function on the curvature in the y direction.

Despite the appearance of the factor of $\cot\theta$ in Eq. (53), $C_{22}(\theta)$ is well behaved in the limit $\theta\to 0$. To see this, note that for small θ,

$$M_x^{(1)}(\theta) \cong R_0 + R_1\theta, \quad (54)$$

where R_0 and R_1 are finite constants. Symmetry demands that $M_x^{(1)}(0)=0$, and thus $R_0=0$. Therefore, in the limit of small θ, the lowest-order term in $M_x^{(1)}$ is proportional to θ. It follows that

$$\lim_{\theta\to 0}\left[\cos\theta\,\cot\theta M_x^{(1)}(\theta)\right] = R_1. \quad (55)$$

The value of the constant R_1 of course depends on the specifics of the crater being considered, but it is finite.

VI. APPLICATION OF THE FORMALISM TO THE SIGMUND MODEL

In this section, we demonstrate explicitly that our crater function formalism yields the exact BH coefficients for the Sigmund model. The crater function for the Sigmund model is given by Eq. (8) of Ref. [37]. For convenience, we will adopt the same notation that was used in that paper [38]. On average, an impact at the origin produces a crater whose negative depth at point $\boldsymbol{r}=x\hat{\boldsymbol{x}}+y\hat{\boldsymbol{y}}+h(x,y)\hat{\boldsymbol{z}}$ is

$$F(x,y,\theta,K_{11},K_{12},K_{22})$$
$$= \frac{\epsilon\Lambda}{(2\pi)^{3/2}\alpha\beta^2}\exp\left(-\frac{1}{2\alpha^2}[a-x\,\sin\theta+h(x,y)\cos\theta]^2\right.$$
$$\left.-\frac{1}{2\beta^2}[x\,\cos\theta+h(x,y)\sin\theta]^2-\frac{1}{2\beta^2}y^2\right). \quad (56)$$

If the distance between the origin and $\boldsymbol{r}$ does not exceed a few times l, then we may set

$$h(x,y) = \tfrac{1}{2}K_{11}x^2 + K_{12}xy + \tfrac{1}{2}K_{22}y^2 \quad (57)$$

in Eq. (56). The dependence of the crater for the Sigmund model on the components K_{ij} of the curvature tensor becomes manifest once Eq. (57) has been inserted into Eq. (56).

For brevity, let

$$D \equiv \frac{a^2\epsilon\Lambda}{(2\pi)^{3/2}\alpha\beta^2}. \quad (58)$$

We readily obtain

$$M_x^{(0)} = D\iint\exp\left(-\frac{1}{2}a_\alpha^2(1-x\,\sin\theta)^2\right.$$
$$\left.-\frac{1}{2}a_\beta^2x^2\cos^2\theta-\frac{1}{2}a_\beta^2y^2\right)dx\,dy$$
$$= De^{-a_\alpha^2/2}\iint\exp\left(-\frac{B_1}{2}x^2+Ax-\frac{a_\beta^2}{2}y^2\right)dx\,dy$$
$$= De^{-a_\alpha^2/2}\frac{2\pi}{a_\beta\sqrt{B_1}}\exp\left(\frac{A^2}{2B_1}\right), \quad (59)$$

and

$$M_x^{(1)} = aDe^{-a_\alpha^2/2}\iint x\,\exp\left(-\frac{B_1}{2}x^2+Ax-\frac{a_\beta^2}{2}y^2\right)dx\,dy$$
$$= \frac{aA}{B_1}M_x^{(0)}. \quad (60)$$

To find C_{11} and C_{22}, we need the partial derivatives of the curvature-dependent moments $M_{K_{22}}$ and $M_{K_{22}}$ with respect to K_{11} and K_{22}, respectively. Since the K_{ij}'s do not depend on x and y, we may exchange differentiation with respect to the K_{ij}'s with integration over x and y. This gives

$$\begin{aligned}\frac{\partial}{\partial K_{11}}M_{K_{11}}\bigg|_{K_{11}=0} &= \iint \frac{\partial}{\partial K_{11}}F(x,y,\theta,K_{11},0,0)\bigg|_{K_{11}=0}dx\,dy \\ &= -aDe^{-a_\alpha^2/2}\iint \exp\left(-\frac{B_1}{2}x^2+Ax-\frac{a_\beta^2}{2}y^2\right)\left(\frac{B_2}{2}x^2+Cx^3\right)dx\,dy \\ &= -aM_x^{(0)}\left(\frac{A^2B_2}{2B_1^2}+\frac{A^3C}{B_1^3}+\frac{B_2}{2B_1}+\frac{3AC}{B_1^2}\right). \end{aligned} \tag{61}$$

Similarly,

$$\begin{aligned}\frac{\partial}{\partial K_{22}}M_{K_{22}}\bigg|_{K_{22}=0} &= \iint \frac{\partial}{\partial K_{22}}F(x,y,\theta,0,0,K_{22})\bigg|_{K_{22}=0}dx\,dy \\ &= -aDe^{-a_\alpha^2/2}\iint \exp\left(-\frac{B_1}{2}x^2+Ax-\frac{a_\beta^2}{2}y^2\right)\left(\frac{B_2}{2}y^2+Cxy^2\right)dx\,dy \\ &= -M_x^{(0)}\frac{a}{a_\beta^2}\left(\frac{B_2}{2}+\frac{AC}{B_1}\right). \end{aligned} \tag{62}$$

We must also compute the derivative of $M_x^{(1)}\cos\theta$ with respect to θ. We obtain

$$\begin{aligned}\frac{\partial\left(M_x^{(1)}\cos\theta\right)}{\partial\theta} &= \frac{\partial}{\partial\theta}\left(\frac{aA}{B_1}M_x^{(0)}\cos\theta\right) \\ &= -aM_x^{(0)}\left[\frac{A\,\sin\theta}{B_1}-\cos\theta\left(\frac{B_2}{B_1}+\frac{6AC}{B_1^2}+\frac{A^2B_2}{B_1^2}+\frac{2A^3C}{B_1^3}\right)\right]. \end{aligned} \tag{63}$$

Finally, we will need the identity

$$\frac{1}{a_\beta^2}\left(B_2+\frac{2AC}{B_1}\right)=\cot\theta\frac{A}{B_1}. \tag{64}$$

Inserting Eqs. (61) and (63) into Eq. (29) yields

$$C_{11}(\theta)=aM_x^{(0)}\left[\frac{A\,\sin\theta}{B_1}-\frac{\cos\theta}{2}\left(\frac{B_2}{B_1}+\frac{6AC}{B_1^2}+\frac{A^2B_2}{B_1^2}+\frac{2A^3C}{B_1^3}\right)\right]. \tag{65}$$

Similarly, inserting Eqs. (60) and (62) into Eq. (53) and applying the identity (64), we have

$$\begin{aligned}C_{22}(\theta) &= -aM_x^{(0)}\left[-\frac{1}{a_\beta^2}\left(\frac{B_2}{2}+\frac{AC}{B_1}\right)+\cot\theta\frac{A}{B_1}\right]\cos\theta \\ &= -M_x^{(0)}\frac{a}{a_\beta^2}\left(\frac{B_2}{2}+\frac{AC}{B_1}\right)\cos\theta. \end{aligned} \tag{66}$$

Note as well that explicit expressions for C_0 and C_1 can be obtained by inserting Eq. (60) into Eqs. (27) and (28). The resulting expressions for C_0 and C_1 and Eqs. (65) and (66) for C_{11} and C_{22} agree with the results obtained by BH for the Sigmund model.

VII. DISCUSSION

The key results of this paper are given by Eqs. (29) and (53). These equations give a means of computing the coefficients C_{11} and C_{22} if the curvature-dependent crater function is known. These coefficients play a key role in determining whether parallel-mode or perpendicular-mode ripples form or if the surface remains flat.

In their 2011 paper, Norris *et al.* [21] gave explicit expressions for C_{11} and C_{22}, namely,

$$C_{11}(\theta)=-\frac{d}{d\theta}\left[M_x^{(1)}(\theta)\cos\theta\right], \tag{67}$$

and

$$C_{22}(\theta)=-M_x^{(1)}(\theta)\cos\theta\,\cot\theta. \tag{68}$$

Our results Eqs. (29) and (53) show that Eqs. (67) and (68) are a good approximation only if the curvature dependence of the crater function is negligible [39].

In the Sigmund model of ion sputtering, the form of the crater depends on the curvature of the surface at the point of impact, despite a statement to the contrary in Ref. [30]. This point has been discussed in detail by Nietiadi and Urbassek

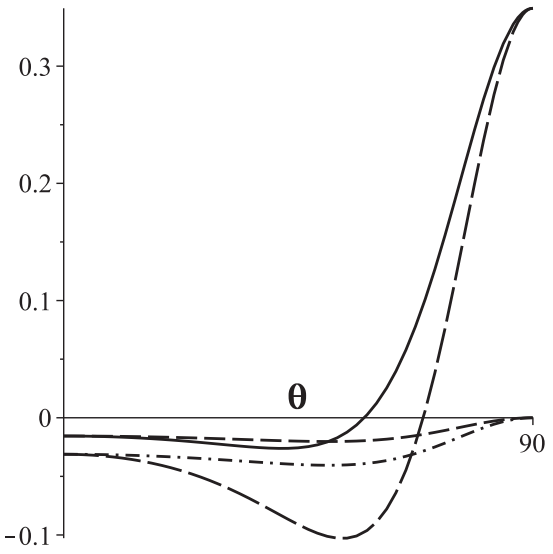

FIG. 2. The coefficients C_{11} and C_{22} as functions of θ for the Sigmund model. The exact results for C_{11} and C_{22} are shown with a solid and dashed curve, respectively. The results obtained for C_{11} and C_{22} if the curvature dependence of the crater function is neglected are shown with long dashes and with a dashed-dotted curve, respectively. The values of a, α, and β employed are for 1-keV Ar^+ bombardment of silicon. The coefficients are in units of $2\sqrt{2\pi}/(\Lambda\epsilon a_\alpha^3 a_\beta)$, and θ is given in degrees.

[36]. The second terms on the right-hand sides of Eqs. (29) and (53) therefore yield nonzero contributions to C_{11} and C_{22}. These contributions were computed explicitly in the preceding section.

For normal-incidence ion bombardment, the values of C_{11} and C_{22} obtained by neglecting the curvature dependence of the crater function [Eqs. (67) and (68)] differ by a factor of 2 from the exact values for the Sigmund model [Eqs. (65) and (66)]. In fact, the result of Norris *et al.* for C_{22} is equal to twice the exact value for all angles of incidence θ.

To get an idea of how much Eq. (67) differs from the exact result for the Sigmund model for nonzero values of θ, see Fig. 2. The values of a, α, and β used in that figure are for 1-keV Ar^+ bombardment of silicon [20]. The ratio of C_{11} as given by Eq. (67) to the exact value is greater than 2 for a broad range of θ values. For $\theta = 45^\circ$, for example, the ratio exceeds 3.5. The angle where the switch from parallel- to perpendicular-mode ripples occurs is 50.8° but, if we use Eqs. (67) and (68), this angle is found to be 66.7°, fully 15.9° higher than the correct value.

Recently, Nietiadi and Urbassek carried out MD simulations of the bombardment of an amorphous silicon target with a normally incident 500-eV Ar^+ beam [36]. They found that the craters for curved surfaces are substantially different than those for a flat surface. These observations and our results for the Sigmund model lead us to the conclusion that the errors incurred by neglecting the curvature dependence of the crater function are typically not small.

The contribution to C_{ii} that comes from the curvature dependence of the crater function is $F_i \cos\theta$, where

$$F_i \equiv -\frac{\partial}{\partial K_{ii}} M_{K_{ii}}\bigg|_{K_{ii}=0} \tag{69}$$

for $i = 1,2$. If K_{ii} is initially zero and then becomes negative, the surface of the solid nears the core of the collision cascade, and the amount of sputtered material increases for an arbitrary choice of target and ion beam. $M_{K_{ii}}$ is a decreasing function of K_{ii} for $i = 1$ and 2 as a result. We conclude that both F_1 and F_2 are positive, which means that the curvature dependence of the crater function yields a *smoothing* contribution to the dynamics that is neglected in Eqs. (67) and (68).

Equations (61) and (62) give the values of F_1 and F_2 for the Sigmund model. It is a simple matter to verify that F_1 and F_2 are indeed positive using these formulas, in accord with our general observation. In addition, for the Sigmund model, F_1 is greater than F_2 for all $\theta > 0$. To see this, note that because the collision cascade is elongated along the direction of the incident ion, the lateral straggling length β is less than the longitudinal straggling length α. Thus, $a_\alpha \equiv a/\alpha < a/\beta \equiv a_\beta$ and $B_1 \equiv a_\alpha^2 \sin^2\theta + a_\beta^2 \cos^2\theta < a_\beta^2$ for $\theta > 0$. The constants A, B_1, B_2, and C are all positive for $\theta > 0$ and $M_x^{(0)} > 0$ as well. Hence

$$\begin{aligned} F_1 &= \frac{a M_x^{(0)}}{B_1}\left(\frac{B_2}{2} + \frac{3AC}{B_1} + \frac{A^2 B_2}{2B_1} + \frac{A^3 C}{B_1^2}\right) \\ &> \frac{a M_x^{(0)}}{a_\beta^2}\left(\frac{B_2}{2} + \frac{AC}{B_1}\right) \\ &= F_2. \end{aligned} \tag{70}$$

For the Sigmund model, therefore, the smoothing effect that comes from the curvature dependence of the crater function is greater for parallel-mode ripples than it is for perpendicular-mode ripples, except of course for the degenerate case of normal-incidence bombardment.

Nietiadi and Urbassek noted that for normal-incidence ion bombardment, the common value of $M_{K_{11}}$ and $M_{K_{22}}$ is a decreasing function of $K_{11} = K_{22}$ for both the Sigmund model and their simulations of sputtering of amorphous silicon [36]. From these observations, they correctly concluded that the curvature dependence of the crater function produces a smoothing effect. However, Nietiadi and Urbassek then went on to assert that this effect "counteracts the main effect of Bradley-Harper theory, since it leads to increased sputtering on crests and decreased sputtering in troughs." In fact, as we have seen, the curvature dependence of the crater function must be taken into account if the exact BH values of the coefficients C_{11} and C_{22} are to be reproduced by the CFF. The smoothing effect produced by the curvature dependence of the crater function is therefore included in the BH theory.

Perkinson *et al.* [35] have recently pointed out some apparent inconsistencies in the coefficients given by Norris *et al.*, Eqs. (67) and (68). Because the expression for C_{11} of Norris *et al.* is a derivative with respect to θ of a function which vanishes at $\theta = 0$ and $\pi/2$, the integral of C_{11} is

$$\int_0^{\pi/2} C_{11}(\theta)d\theta = -M_x^{(1)}(\theta)\cos\theta\Big|_{\theta=0}^{\theta=\pi/2} = 0 \tag{71}$$

for their theory. Additionally, using expressions (67) and (68) of Norris *et al.*, we obtain

$$C_{11}(\theta) = \frac{d}{d\theta}(C_{22}\tan\theta). \tag{72}$$

The experiments of Perkinson *et al.* provide evidence that the actual values for C_{11} and C_{22} do not satisfy either Eq. (71) or (72). This again suggests that the errors incurred by neglecting the curvature dependence of the crater function are significant. When one includes the curvature dependence, however, Eqs. (29) and (53) result, and Eqs. (71) and (72) do not apply. Our CFF therefore does not suffer from the same difficulties as that of Norris *et al.* [21].

The experimental results of Perkinson *et al.* indicate that there is "a surfeit of stability relative to instability compared to the prediction of crater-function theory," i.e., the actual values of C_{11} and C_{22} are larger than the theoretical values obtained using Eqs. (67) and (68). It seems likely that this discrepancy was the result of omitting the smoothing effect of the curvature dependence of the crater function.

As Eq. (27) shows, the crater function for a flat surface is all that is needed to compute C_0. Our expression for C_0 agrees with that of Norris *et al.* as a consequence. Our extended CFF also yields an expression for C_1, Eq. (28). Norris *et al.* did not give an explicit formula that relates C_1 to a crater function moment [21]. This coefficient is needed if one wishes to find the velocity with which parallel-mode ripples propagate over the solid surface.

Norris, Brenner, and Aziz introduced their CFF in 2009 but did not apply it to estimate the coefficients in the EOM for a particular target material or choice of ion beam [30]. Subsequently, Norris *et al.* carried out MD simulations of the bombardment of a flat silicon surface with 100- and 250-eV Ar^+ ions and then used Eqs. (67) and (68) to obtain estimates of C_{11} and C_{22} [21].

The results of Norris *et al.* have some puzzling aspects. For angles of incidence θ below a critical value θ_c, the surface remains flat. For $\theta > \theta_c$, on the other hand, ripples develop as the bombardment proceeds. The experimental value of θ_c Norris *et al.* obtained for 250-eV ions (48°) is approximately 10° larger than the theoretical value they obtained. Moreover, for $\theta = 50°$, the measured ripple wavelength was roughly twice as large as the theoretical value. The difference between the measured and the theoretical wavelengths declined for larger values of θ but remained appreciable up until θ had reached 65°. Finally, a switch from parallel-mode ripples to perpendicular-mode ripples was observed for incidence angles near grazing in the experiments of Norris *et al.*, but no such transition was found by inputting their MD results into Eqs. (67) and (68).

Plausible explanations for these discrepancies between theory and experiment emerge if the curvature dependence of the crater function is taken into account. The smoothing effect of the curvature dependence of the crater function clearly increases the theoretical value of θ_c. Moreover, the wavelength of parallel-mode ripples is inversely proportional to $|C_{11}|^{1/2}$, and so when the contribution to C_{11} that comes from the curvature dependence of the crater function is included, the predicted wavelength increases. Finally, recall that for the Sigmund model the curvature dependence of the crater function has a greater smoothing effect on parallel-mode ripples than it does for perpendicular-mode ripples. It seems likely that this is also true for Ar^+ bombardment of silicon since the Sigmund model provides a good description of the spatial distribution of the deposited energy [40]. It is therefore possible that if the curvature dependence of the crater function had been taken into account by Norris *et al.* in their theoretical work, then they might have found a transition between parallel- and perpendicular-mode ripples as θ nears 90° [41].

If the correct formulas (29) and (53) are to be used in combination with MD simulations to obtain accurate estimates of C_{11} and C_{22}, it is not sufficient to find the crater function for a flat surface. Instead, to find C_{11}, craters on a curved surface of the form $h(x,y) = K_{11}x^2/2$ must be found for a range of small values of K_{11} so that the derivative $\partial M_{K_{11}}/\partial K_{11}$ can be computed for $K_{11} = 0$. Naturally, an analogous statement applies to determining C_{22}. In that case, craters on a surface that has the form $h(x,y) = K_{22}y^2/2$ are needed. This means that the computational resources necessary to find accurate values of the coefficients C_{11} and C_{22} are considerably greater than previously thought.

VIII. CONCLUSIONS

In principle, the crater function F depends on the entire shape of the surface in the vicinity of the point of impact. In this paper, we extended the crater function formalism to include the dependence of F on the curvature of the surface at the point of impact. Explicit expressions for the constant coefficients in the continuum equation of motion were derived; these reduce to the results given by Norris *et al.* [21] *only* if the curvature dependence of the crater function is negligible. Our extended crater function formalism yields the exact coefficients for the Sigmund model of ion sputtering. In contrast, if the curvature dependence of the crater function is neglected, substantial errors in the estimated values of the coefficients typically ensue.

Our results show that accurately estimating the coefficients in the equation of motion using craters obtained from molecular dynamics simulations will require significantly more computational power than was previously thought. They also lead us to question the reliability of the coefficient estimates that have been obtained using the version of the crater function formalism in which the curvature dependence of the crater function is neglected.

ACKNOWLEDGMENTS

We have benefited from stimulating discussions and correspondence with H. Hofsäss, K. F. Ludwig, S. A. Norris, and P. D. Shipman. R.M.B. would like to thank the National Science Foundation for its support through Grant No. DMR-1305449.

[1] For a review, see J. Muñoz-García, L. Vázquez, R. Cuerno, J. A. Sánchez-García, M. Castro, and R. Gago, in *Toward Functional Nanomaterials*, edited by Z. M. Wang (Springer, Dordrecht, 2009).

[2] S. Facsko, T. Dekorsy, C. Koerdt, C. Trappe, H. Kurz, A. Vogt, and H. L. Hartnagel, Science **285**, 1551 (1999).

[3] F. Frost, A. Schindler, and F. Bigl, Phys. Rev. Lett. **85**, 4116 (2000).

[4] Q. Wei, X. Zhou, B. Joshi, Y. Chen, K.-D. Li, Q. Wei, K. Sun, and L. Wang, Adv. Mater. **21**, 2865 (2009).
[5] M. Fritzsche, A. Muecklich, and S. Facsko, Appl. Phys. Lett. **100**, 223108 (2012).
[6] L. Bischoff, W. Pilz, and B. Schmidt, Appl. Phys. A **104**, 1153 (2011).
[7] L. Bischoff, K.-H. Heinig, B. Schmidt, S. Facsko, and W. Pilz, Nucl. Instrum. Methods Phys. Res., Sect. B **272**, 198 (2012).
[8] R. M. Bradley and J. M. E. Harper, J. Vac. Sci. Technol. A **6**, 2390 (1988).
[9] P. Sigmund, J. Mater. Sci. **8**, 1545 (1973).
[10] R. Cuerno and A.-L. Barabási, Phys. Rev. Lett. **74**, 4746 (1995).
[11] M. A. Makeev, R. Cuerno, and A.-L. Barabási, Nucl. Instrum. Methods Phys. Res., Sect. B **197**, 185 (2002).
[12] M. Castro, R. Cuerno, L. Vazquez, and R. Gago, Phys. Rev. Lett. **94**, 016102 (2005).
[13] J. Muñoz-García, R. Cuerno, and M. Castro, Phys. Rev. B **78**, 205408 (2008).
[14] V. B. Shenoy, W. L. Chan, and E. Chason, Phys. Rev. Lett. **98**, 256101 (2007).
[15] G. Carter and V. Vishnyakov, Phys. Rev. B **54**, 17647 (1996).
[16] M. Moseler, P. Gumbsch, C. Casiraghi, A. C. Ferrari, and J. Robertson, Science **309**, 1545 (2005).
[17] B. Davidovitch, M. J. Aziz, and M. P. Brenner, Phys. Rev. B **76**, 205420 (2007).
[18] N. Kalyanasundaram, M. Ghazisaeidi, J. B. Freund, and H. T. Johnson, Appl. Phys. Lett. **92**, 131909 (2008).
[19] N. Kalyanasundaram, J. B. Freund, and H. T. Johnson, J. Phys.: Condens. Matter **21**, 224018 (2009).
[20] C. S. Madi, E. Anzenberg, K. F. Ludwig, Jr., and M. J. Aziz, Phys. Rev. Lett. **106**, 066101 (2011).
[21] S. A. Norris, J. Samela, L. Bukonte, M. Backman, F. Djurabekova, K. Nordlund, C. S. Madi, M. P. Brenner, and M. J. Aziz, Nat. Commun. **2**, 276 (2011).
[22] M. Castro and R. Cuerno, Appl. Surf. Sci. **258**, 4171 (2012).
[23] S. A. Norris, Phys. Rev. B **85**, 155325 (2012).
[24] S. A. Norris, Phys. Rev. B **86**, 235405 (2012).
[25] M. Castro, R. Gago, L. Vázquez, J. Muñoz-García, and R. Cuerno, Phys. Rev. B **86**, 214107 (2012).
[26] O. Bobes, K. Zhang, and H. Hofsäss, Phys. Rev. B **86**, 235414 (2012).
[27] H. Hofsäss, O. Bobes, and K. Zhang, in *Application of Accelerators in Research and Industry: Twenty-Second International Conference*, edited by F. D. McDaniel, B. L. Doyle, G. A. Glass, and Y. Wang, AIP Conf. Proc. No. 1525 (AIP, New York, 2013), p. 386.
[28] Z. Yang, M. Lively, and J. P. Allain, Nucl. Instrum. Methods Phys. Res., Sect. B **307**, 189 (2013).
[29] W. Möller, Nucl. Instrum. Methods Phys. Res., Sect. B **322**, 23 (2014).
[30] S. A. Norris, M. P. Brenner, and M. J. Aziz, J. Phys.: Condens. Matter **21**, 224017 (2009).
[31] In practice, an average over impact points is performed in an MD simulation. If the surface is not flat, then these impact points would have to be close enough together for the surface curvature to be very nearly the same for each selected point of impact.
[32] S. A. Norris, J. Samela, M. Vestberg, K. Nordlund, and M. J. Aziz, Nucl. Instrum. Methods Phys. Res., Sect. B **318**, 245 (2014).
[33] M. Z. Hossain, K. Das, J. B. Freund, and H. T. Johnson, Appl. Phys. Lett. **99**, 151913 (2011).
[34] C. C. Umbach, R. L. Headrick, and K.-C. Chang, Phys. Rev. Lett. **87**, 246104 (2001).
[35] J. C. Perkinson, E. Anzenberg, M. J. Aziz, and K. F. Ludwig, Phys. Rev. B. **89**, 115433 (2014).
[36] M. L. Nietiadi and H. M. Urbassek, Appl. Phys. Lett. **103**, 113108 (2013).
[37] R. M. Bradley, Phys. Rev. B **84**, 075413 (2011).
[38] Note that the θ used in Ref. [37] is minus the θ employed here and in Ref. [21].
[39] The crater function defined by Norris *et al.* [21] differs from ours by a sign. This leads to the minus sign on the right-hand side of Eqs. (67) and (68).
[40] M. Z. Hossain, J. B. Freund, and H. T. Johnson, J. Appl. Phys. **111**, 103513 (2012).
[41] Hossain *et al.* found a transition between parallel- and perpendicular-mode ripples using their MD results, even though they neglected the curvature dependence of the crater function [33].